Contactless CAN Interface for rail topologies

Derk Wesemann (derk.wesemann@hs-owl.de), Institut Industrial IT (inIT)

Stefan Witte (stefan.witte@hs-owl.de), Hochschule Ostwestfalen Lippe

Helmut Beikirch (helmut.beikirch@uni-rostock.de), Universität Rostock

Contactless interfaces are essential to different applications which rely on physical robustness and / or high modularity and movability. This work presents a solution for direct conversion of CAN signals for contactless capacitive coupling over an air gap. The coupling distances are short (in the range of less than 1 mm), but can be extended by a supporting rail which contains coupling electrodes and conductors to deliver the signals also over larger distances. A modulation scheme is implemented to maintain the functionality of dominant and recessive bit status. No additional controller is needed; the transceiver module replaces the CAN transceiver typically added to any microcontroller.

Introduction

Wireless CAN implementations are already available and often realized using alternative protocols like Bluetooth, GSM or WLAN, where the wireless part is integrated in the form of a gateway [1], [2]. These gateways connect CAN network segments, acting as bridges. If one wants to implement single contactless connected CAN devices, these bridges have several drawbacks. Separate controllers are needed for each device, leading to additional latency, energy consumption and cost.

This work presents a solution with a novel contactless transceiver replacing the CAN-transceiver typically added to a microcontroller, leading to a transparent alternative physical layer without the need for modification of the microcontroller in means of software or hardware.

The targeted application of these transceivers is a contactless backbone for industrial automation components, where its implementation in combination with an also contactless energy supply (inductively coupled) reduces the wiring complexity and mechanical stress for connectors [3].

Physical characteristics

Contactless communication methods can rely on different physical principles. Signals are transmitted over an electromagnetic field, which can take the form of electromagnetic coupling between two or more antennas, inductive coupling between coils, capacitive coupling between electrodes or also by light emission and detection [4]. In this work, the transmission of signals by means of capacitive coupling will be under further investigation, since it addresses the underlying project's needs.

Capacitive coupling relies on a considerable capacitance to be formed between two adjacent electrodes. With limited space available in most cases, only small capacitances can be realized, due to the coupling distance and small area.

Since a bus structure needs to be realized and not only a single one-to-one communication situation, a more complex physical setup is to be implemented, if more than two network participants want to communicate using CAN. The proposed layout consists of a supporting rail structure, carrying stripline conductors which serve as coupling electrodes at

occupied positions. Figure no. 1 illustrates this setup for two bus nodes.

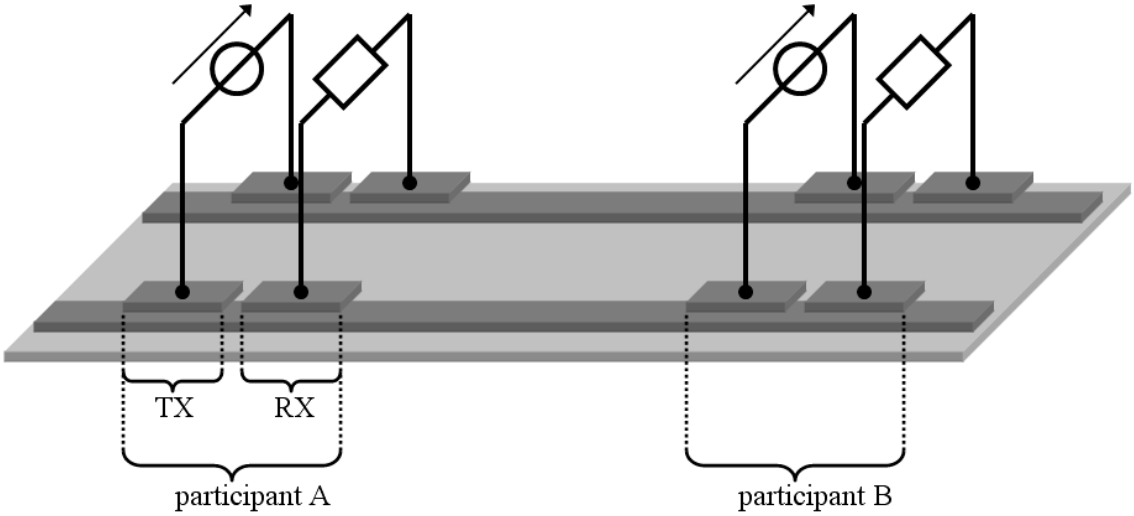

Figure 1: Capacitively coupled bus structure

The signals can couple from any participant onto the rail and start propagating into both directions, therefore a signal emitted by one participant can be read at any position on the rail. The needed energy for the signal is relatively low, since radiation is not intended and only low power can be coupled over small capacitances at these comparable low frequencies. The signal needs to transverse an air gap two times, leading to a total capacitance half the size of one coupling capacitance between one participant and the rail, assuming identical mounting conditions.

Modulation scheme

Like any other wireless transmission, the contactless capacitive coupling benefits from signal modulation instead of a baseband transmission. The baseband approach was tested and omitted, since due to the nature of the coupling capacitance, only the edges of a digital signal can be detected on the receiver side, while the constant signals values during bit-time give no signal contribution after a capacitor. This rather simple edge detection would lead to sufficient results for general digital signals, but lacks the possibility to create a dominant signal level, which is absolutely necessary for a CAN implementation.

As the most basic modulation method, a binary ASK (amplitude shift keying), often also referred to as OOK (On-Off-Keying) was chosen. The different bit states are described by a present or missing carrier; in this case an active carrier represents the dominant bit, and a missing carrier the recessive bit. This way, the function of a dominant bus status can be maintained. The relation is described in illustration 2, showing an input signal given by a microcontroller and the corresponding modulated waveform.

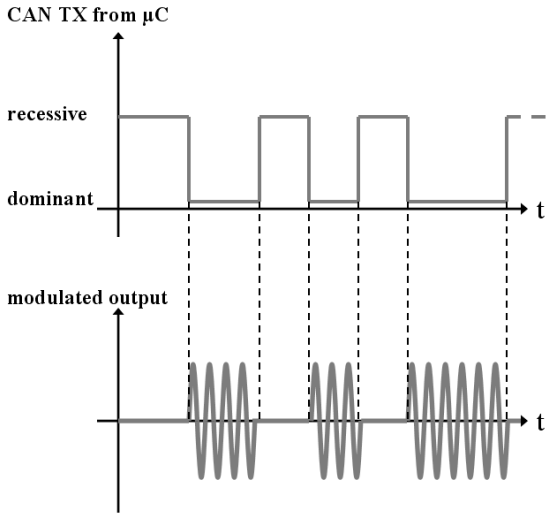

Figure 2: OOK modulation for CAN

Errors can occur by external signals in a similar frequency range, if they are sufficiently high for the receiver to detect a

dominant level. This demands a proper filtering on the hardware level as well as a well chosen modulation frequency.

Transmitter

For creating an OOK-Signal, a transmitter basically needs to include an oscillator and a switch. The digital signal controls the switch, and the output oscillates with the carrier frequency, depending on the digital input to the switch. Due to CAN logic levels, a low signal on the input needs to create an oscillation, while a high input level should leave the output flat. The transmitter needs to connect to the common microcontroller outputs; therefore it should work for both 3.3 and 5 Volt logic. A basic block diagram is shown in figure no. 3.

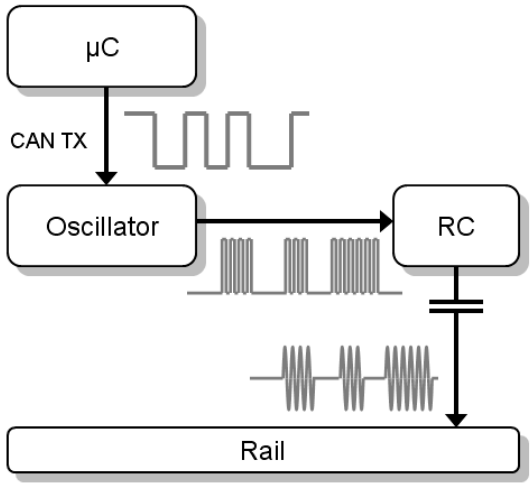

Figure 3: Transmitter setup and signals

An easy solution for implementing such a transmitter stage could be found with the LTC6905 from Linear Technology. It consists of an integrated oscillator with an output-enable-function, all combined in an SOT-23 housing, leaving a very small footprint. For the output is a rectangular signal, an RC-Circuit needs to be included between the IC and the coupling capacitances, leading to a more sine-like signal which passes the coupling electrodes with only small distortion. The IC itself can be tuned to three different frequencies by external circuitry, which is realized by setting a divider of 1, 2 or 4 to a fixed internal frequency. The different available types cover a range from 20 to 133 MHz, while 33 MHz was chosen for implementation. The frequency stability, normally a hard criterion for modulated signals, is not very critical in this application, since the receiver will react to any signal within a input filter range.

Receiver

The receiver needs to detect a signal with one specified frequency and set its output depending on whether the signal is present or not. This kind of detection circuitry can be found in most wireless communication setups under the term RSSI (receiver strength signal indicator). Unfortunately, the available components in this area are suitable for high frequencies, but bear only very slow output signals, since they are not intended to be carrying payload data. In short notice: The rise and fall times of the output disqualifies these devices for high speed data transmission.

For the receiver, no single chip solution could be found. Instead, the necessary stages for filtering, amplification and decision were implemented with discrete elements. The block diagram in illustration no. 4 identifies the receiver components.

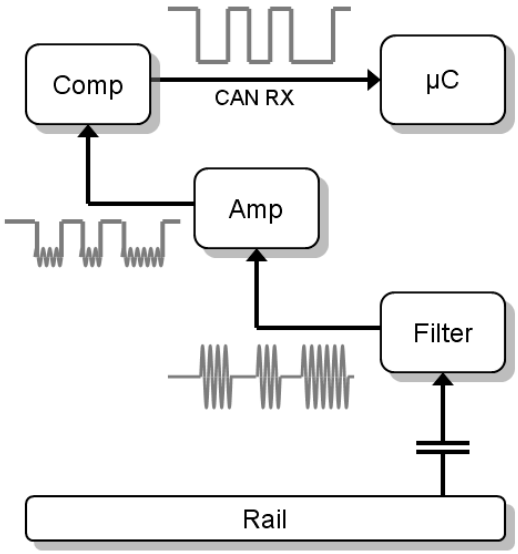

Figure 4: Receiver setup and signals

The filter stage is designed as a T-bandpass with a center frequency

according to the transmitter's operating frequency. It consists of three L/C-circuits, creating a filter of 3rd order.

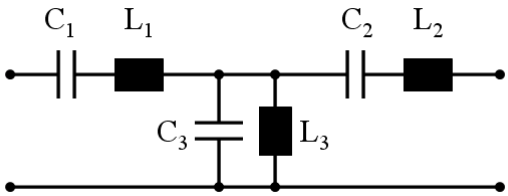

Figure 5: Filter circuit, T-type

The filter was designed for 33 MHz center frequency, according to the modulation frequency. Simulation was run using PSPICE, while measurements were performed with a network analyzer. The following values were used:

Table 1: Filter components

Part	Value	Unit
C1	22	pF
C2	22	pF
C3	1	nF
L1	1	µH
L2	1	µH
L3	22	nH

The simulation result is shown in figure no. 6, compared to the measured results. For higher frequencies, the damping performance differs significantly from the simulation. This effect can be explained by the simulation containing ideal components only; with a more proper choice of real components, this difference might be reduced.

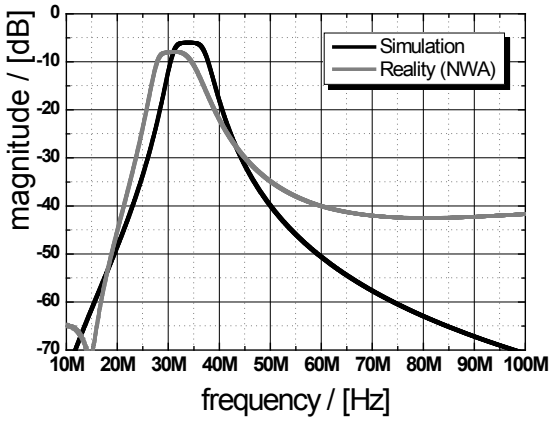

Figure 6: Filter frequency characteristic

While the filter allows high slew rates (18 dB/octave), the damping rate is fairly high (8 dB), which needs to be compensated by the following first amplification stage.

The amplification stage is realized with two transistors in emitter configuration. The used transistors are of type BFS17, which are suitable for frequencies up to 1 GHz, and deliver a typical current gain of 90. The first amplification stage performs amplification only. The second stage is set to an operating point near the transistor's conducting border. This way, its amplification is near the factor 1, but it has the advantage that the transistor only conducts when the signal is above the threshold. It blocks while the signal is not detected (or simply too low to be detected), binding the output to the supply voltage level. This way, an almost rectangular shaped signal can already be generated, like depicted in figure no. 4.

To complete the A/D-conversion process, the amplification stage is followed by a comparator. The threshold is externally adjustable and should be chosen in a way to optimally distinguish between the conducting and non-conducting condition of the second amplification stage. Additionally, the circuitry comprises a positive feedback line, allowing a hysteresis to be implemented which further minimizes comparison errors.

Simulation results

Before building any hardware, the transmission scenario was modelled using again a PSPICE environment. The model consists of one transmitter, the conducting rail and one receiver, resembling one transmission path. A continuous rectangular square wave signal was chosen as the input and mixed with the carrier signal (33 MHz sinusoid). The conducting rail was simulated with two transmission line models, one for each stripline, with the values for the line impedance being derived from the geometrical layout. Circuitries and components for both amplifications stages and the comparator were chosen to achieve the best match between input and output signals. The signal waveforms before and after the comparator are shown in illustration no. 7.

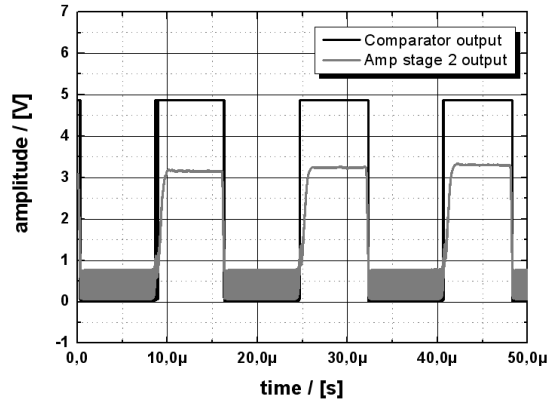

Figure 7: Simulation results receiver side, for square wave input

Test application

The contactless transceivers have been tested together with microcontrollers of the type HCS12. The controllers and transceivers were powered with 5V by two different supplies, one for each participant.

The test application consists of two CAN network participants mounted on an installation rail, according to the previously described setup. Each participant comes with a total width of 22 mm, in combination with the rail width of 35 mm, this leads to an available coupling area of 770 mm². Since the data transmission shares this space with an inductive energy supply which is not further described in this work, only a smaller area is really usable. Due to the layout requirements from the other embedded functional components, the coupling electrodes were chosen with a size of 4.4 x 9.2 mm². With respect to the coupling distance of 0.1 mm and polyethylene as the separating material, this leads to a coupling capacitance of 8.6 pF, theoretically. The geometries of the rail and nodes are shown in figure no. 8.

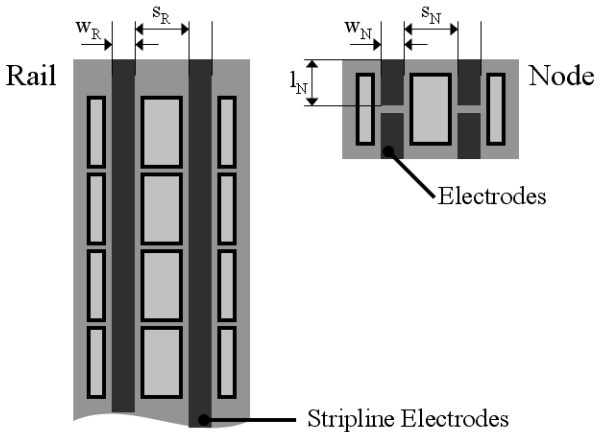

Figure 8: Rail and node geometry

The rail covers a total length of 330 mm, the other geometrical values are given in table 2:

Table 2: Dimensions for rail and node conductors

Dimension	Value	Unit
w_R	4.4	mm
s_R	4.6	mm
w_N	4.4	mm
s_N	4.6	mm
l_N	9.2	mm

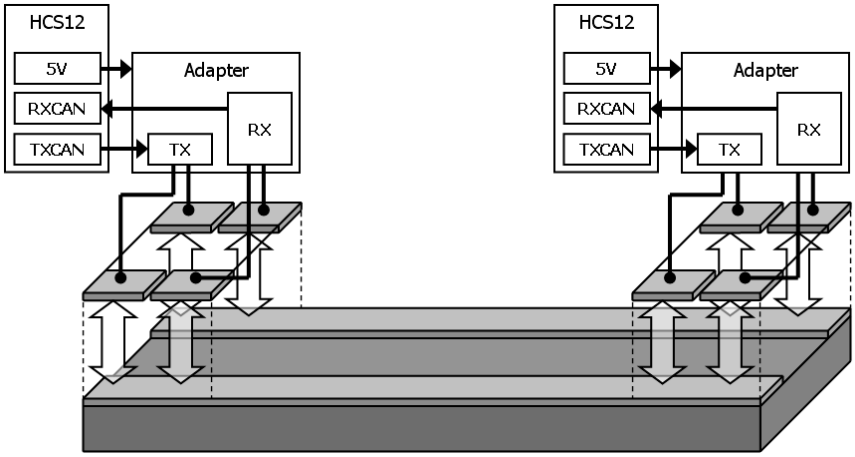

Figure 9: Test application with rail, controllers and transceivers

Results

The CAN signal could be reconstructed correctly at node 2, enabling a complete CAN transmission including acknowledge between the two nodes. One frame with one byte payload (0xAA hexadecimal) was transmitted exemplary. Taking a look at the receiver side, the signal after the first amplification stage is shown in figure no. 10.

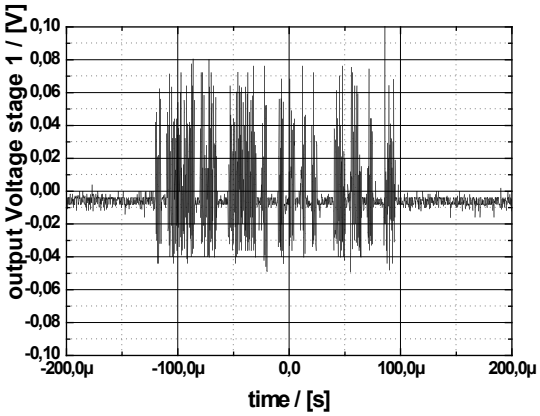

Figure 10: Amplified signal after first stage

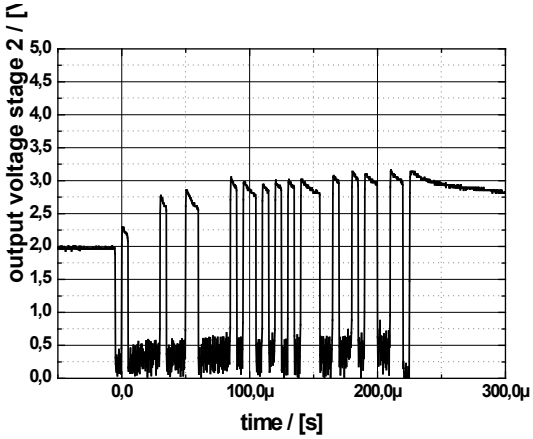

Figure 11: Signal after second amplification stage

With the signal after the second amplification stage (figure no.11), a reconstruction can be easily performed with the comparator. Original and received signal are shown in figure no. 12.

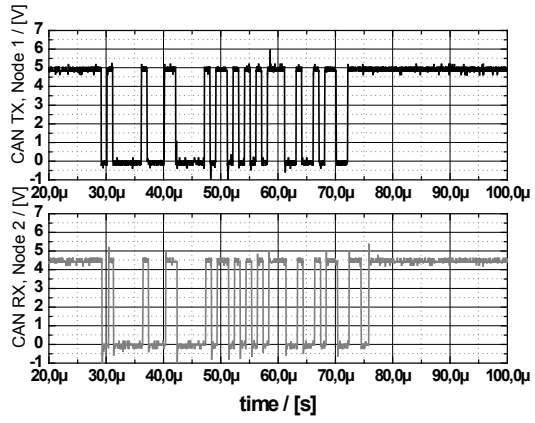

Figure 12: Original and received signal

Of particular interest was the overall system timing, especially the delay of the transmission, which limits the total distance a CAN network is able to cover. Commonly available CAN transceivers employ a total loop delay of 90 – 190 ns (Texas Instruments SN65HVD1050, [5]), so the goal was not to exceed these values. Figure no. 13 shows the results for the falling edge in the beginning of a transmission.

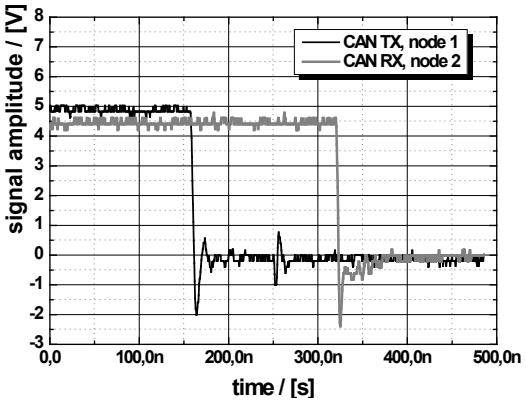

Figure 13: Signal delay between transmitter and receiver

It can be observed, that a total end-to-end delay of roughly 160 ns could be achieved at a data rate of 1 MBit/s, which is comparable to the guaranteed value of commercially available components. The distance between both nodes was less than 30 cm.

References

[1] Kongezos, V.K.; Allen, C.R.; "Wireless communication between AGVs (autonomous guided vehicles) and the industrial network CAN (controller area network)," *Robotics and Automation, 2002. Proceedings. ICRA '02. IEEE International Conference on* , vol.1, no., pp. 434- 437 vol.1, 2002

[2] Johanson, M.; Karlsson, L.; Risch, T.; "Relaying Controller Area Network Frames over Wireless Internetworks for Automotive Testing Applications," *Systems and Networks Communications, 2009. ICSNC '09. Fourth International Conference on* , vol., no., pp.1-5, 20-25 Sept. 2009

[3] Wesemann, D.;, Michels, J.S.; Schmidt, H.P.; Witte, S;, „Kontaktlose Energie- und Datenübertragung für anreihbare Automatisierungskomponenten“, *VDI Kongress Automation 2010*, June 2010, Baden Baden

[4] Kyung-Rak Sohn; Hee-Jin Lee; Yeun-Ju Kim; , "Wireless CAN communications based on white LED," *Ubiquitous and Future Networks (ICUFN), 2011 Third International Conference on* , vol., no., pp.127-130, 15-17 June 2011

[5] Texas Instruments, “EMC Optimized CAN Transceiver”, March 2010. http://www.ti.com/lit/ds/symlink/sn65hvd1050.pdf [Accessed Nov. 2011]

Derk Wesemann
Institut Industrial IT (inIT)
Langenbruch 6
32657 Lemgo
Tel: +49 5261 702589
Fax: +49 5261 702137
derk.wesemann@hs-owl.de
www.init-owl.de

Stefan Witte
Hochschule Ostwestfalen-Lippe
Liebigstraße 87
32657 Lemgo
Tel: +49 5261 702116
Fax: +49 5261 702137
stefan.witte@hs-owl.de
www.hs-owl.de

Helmut Beikirch
Universität Rostock
Albert-Einstein-Str. 2
18051 Rostock
Tel: +49 381 4987203
Fax: +49 381 4987202
helmut.beikirch@uni-rostock.de
www.igs.uni-rostock.de